

---

[entry]none/global



Applied Physics Master Lab:

Diamonds for Sensing Applications

Cristian Medina  
Simon Stephan

conducted from 28.05.2018 to 01.06.2018

---

## Abstract

Optical detection of electron spin resonances of nitrogen-vacancy (NV) centers in diamond [14, 15, 42]. This system offers the possibility to detect magnetic fields with an unprecedented combination of spatial resolution and magnetic sensitivity [43, 41, 13, 42, 44], in a wide range of temperatures (from 0 K to well above 300 K), opening up new frontiers in biological [14, 45, 46] and condensed-matter [14, 47, 48] research. Over the last few years, researchers have developed techniques for scanning magnetometry using nanoscale imaging techniques in bulk diamond [15, 42, 49], as well as in nanodiamonds [50, 51, 52] combined with scanning probe techniques [14, 53]. Sensors employing ensembles of NV centers promise even higher sensitivity and the possibility to map out all vector components of the magnetic field [13, 12], and pilot NV-ensemble magnetometers have recently been demonstrated by several groups [48, 47, 54, 44]

# Contents

<b>1</b>	<b>Introduction</b>	<b>1</b>
<b>2</b>	<b>Theoretical Background</b>	<b>2</b>
2.1	Colour Centres . . . . .	2
2.2	NV-Centres in Diamonds . . . . .	2
2.3	Optically Detected Magnetic Resonance . . . . .	2
<b>3</b>	<b>Experimental Set-up and Procedure</b>	<b>3</b>
3.1	Set-Up . . . . .	3
3.2	Calibration . . . . .	3
3.2.1	conversion factor camera . . . . .	3
3.2.2	Electronic components . . . . .	3
3.3	Measurements . . . . .	3
<b>4</b>	<b>Evaluation</b>	<b>6</b>
4.1	Calibration . . . . .	6
4.1.1	Laser Power . . . . .	6
4.1.2	Optical Spectrometer . . . . .	6
4.1.3	ODMR calibrations . . . . .	6
4.2	Size of the Diamonds . . . . .	7
4.3	Fluorescence Spectrum . . . . .	7
4.4	ODMR Measurements . . . . .	7
<b>5</b>	<b>Summary and Discussion</b>	<b>12</b>
<b>6</b>	<b>Appendix</b>	<b>13</b>

# 1 Introduction

Diamonds are not just known and appreciated by their beauty but also for its important technical properties like their mechanical hardness which they mainly get from their crystal structure. Nevertheless there are defects in their lattice structure which enable us to use diamonds more variously. Colour centres, for example, are fluorescent lattice defects which can be used for many sensing applications [**anleitung**]. In this experiment we will examine the properties of the so-called nitrogen vacancy (NV) centre and its sensitivity to magnetic fields.

Colour centres (CC) are regular spacing in the lattice that absorbs a particular colour in light. This not just gives a special colour to the diamond but also relates to more interesting properties like fluorescence. where the lattice atoms get lifted into an excited state and then decaying back into the ground state by emitting a photon with a wavelength in the visible range. The fluorescence here examined are the NV-centres that can be used to detect magnetic fields giving place to Optical Detection Magneto resonance or ODMR.

ODMR is done using the measurement method in which the NV-centres are excited by microwaves which leads to a loss in fluorescence at a certain microwave frequency. The recorded frequency spectrum in a frequency range around that frequency depends on the external magnetic field.

Also the fluorescence spectrum of the diamond as well as its size will be measured using an optical spectrometer and a CCD camera.

## 2 Theoretical Background

In the following some physical concepts needed for the understanding of this experiment are explained.

### 2.1 Colour Centres

Diamond structure is a well known and studied in crystallography. Its lattice consists in a cubic structure based on 8 Carbon atoms, two tetrahedrally bonded atoms in each primitive. The diamond lattice is basically two face-centered cubic lattices, being the face centers (FCC) atom on one cell the vertex of the other. Since there are two identical atoms per unit cell, there is no absorption of photon in the IR-region. This means that a pure diamond can not have fluorescence properties (in first order) but this property can be achieved with changes due to impurities in the structure. These properties are called Colour centers.

Colour centres (CC) are a kind of point defects in crystal structures which contain an electron that absorbs light of certain wavelengths. This basic defect in the regular spacing of atoms within a solid that absorbs visible light of a particular colour, lending a characteristic colour to the solid.

There are more than 100 luminescent defects in diamond. Another name that is known is F-centre (German Farbe, "colour"), results from the absence of a negatively charged ion from a particular point in an ionic solid. This vacancy, which acts like a positively charged particle, attracts and traps an electron, and their combination constitutes an Colour-centre. One of the most abundant and also studied one is the Nitrogen related defects, or Nitrogen-Vacancy centers (NV), because nitrogen is a prominent impurity in the material. In next section we will talk in more detail about its properties.

### 2.2 NV-Centres in Diamonds

The NV-centers are a defect or impurity in the diamond structure, where two carbon atoms in the secondary fcc are replaced, one by a nitrogen atom and the second one by a vacant. The single substitutional nitrogen has an infrared mode of vibration. Nitrogen aggregates are, pairs of neighbouring substitutional atoms, the nitrogen aggregates, and its neighbours that lead to different combinations (eighth total usually labelled according to corresponding Miller indices) in the lattices that have distinct infrared spectra. In the next figure, the first fcc lattice of the diamond is shown and in the second structure one of the carbons was replaced by the N. NV-center can exist in two charge states, the neutral  $NV^0$  state and the negatively charged  $NV^-$  state that have different energy levels and allow transition.

The most interesting properties of the NV centers is its absorption and emission fluorescence at red region, property fundamental that will be studied in this experiment, and is mostly due to physical effects by the magnetic moment. A simplified quantum structure of the NV center can be seen in the fig .... where the ground state and excited state are constructed by triplet states with a distance of 1.945 eV in between, here called  $^3A_2$  and  $^3E$  respectively. The main radiative connection between the ground state and the excited state is due to the zero phonon line (ZPL). For the negatively charged NV center, this transition contributes to a wavelength of  $\lambda_{zpl} = 637 \text{ nm}$  and has a lifetime of 10-30 ns. (To observe the ZPL, a simple absorption emission process was done with a 519nm laser was done, identify this peak at... .) An additional process from the excited state is a nonradiative emission into the metastable singlet state  $|s\rangle$ . This can either occur from the state  $|e,ms\rangle$ , in a weak non-radiative decay.

### 2.3 Optically Detected Magnetic Resonance

## 3 Experimental Set-up and Procedure

### 3.1 Set-Up

### 3.2 Calibration

#### 3.2.1 conversion factor camera

The strip was measure with a calibrator at  $1.2 \pm 0.1$  mm and the camara used was a Thorlabs CCD camera with dimentions of 1280x1024 pixels, each pixel with  $5.2 \times 5.2 \mu\text{m}$  according to the manufacturer. In order to know the actual resolution of our microscope a calibration was done based on the magnification and calibration factor of the set up. Theoritically our  $C_f$  can be calculated as:

$$C_f = \frac{1px \cdot M}{d_p} = 1552px/mm \quad (1)$$

Where  $M$  is the magnification and  $d_p$  is the pixel sizes. And with a Magnification icual to the lenses used for the confocal setup is equal to the magnification  $M = f2/f1 = 8$ . In this case the tool of Thorlab's software was used to determine and measure the width of the microstrip. Using the equation above and the respective measmente we denote that  $C_f = 1346 \text{ px/mm}$ , with a magnification factor close to  $M = 7X$ .

#### 3.2.2 Electronic components

In order Performe our ODMR, is crucial to determine the amount of microwave power deployed into the microstrip and the diamonds. we can not have an absolut power that is been plugging into the set up. The microstrip by defoult have some transimtion  $T_{Ms}$  and refleccions  $R_{Ms}$  that are unkown. For this a power coupler was added to the setup and four meassment with diferents arranges where performed as shown in the fig... First, the power coupler was conected to the DSA in out- out possition to knoe the transmitio of it,  $T_{cpl}$ . on the other hand the secon setup is an Out conection to the DSA and help to determine the reflection of the CPL  $R_{cpl}$ . for the thirt and fouth display, the mmicrostrip was added, in the Out-Out possition ( CPL-DSA), messurion the Reflection  $R_{cpl-Ms}$  and transimtion  $T_{cpl-Ms}$  of the hole set.

The DSA was set at 0 Dbm and a sweep centered at 2.8GHz frequency. A  $50\Omega$  resistance was used for the losses ends as shown. The next figure display the four signals of the diferent arranges.

The total transimtion and reflection ws simply calculated by a sustraction of the Ms trasmission in the diferent processes as next.

$$T_{Ms} = T_{cpl-Ms} - T_{cpl}R_{MS} = R_{cpl-Ms} + T_{cpl} - R_{cpl} \quad (2)$$

The atenuation in this cases for the transmiition remains close to cero, specially in the center of the sweep while the reflection as shown reducs drastricly. This gives us the facts that the power trasmitted is close to the 0dBm used in the DSA and few of it is been reflected.

### 3.3 Measurements

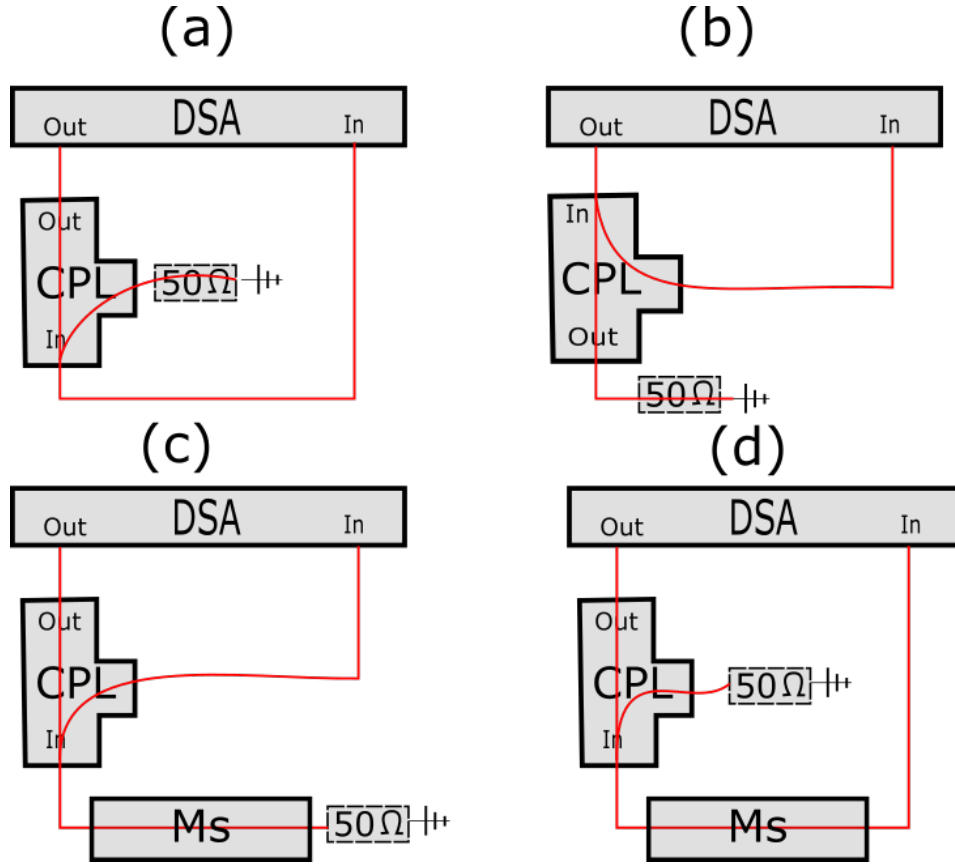


**Figure 1:** (A) CPL conected to the DSA in Out-Out direction meassuring  $T_{cpl}$ , (b) Cpl conected in Out-In sequence and meassuring  $R_{cpl}$ , (c) CPL and microstrip conected in Out-Out mode and meassuring the  $R_{cpl-MS}$  (d) CPL and Microstrip conected in Out-Out moded and meassuring  $T_{cpl-MS}$

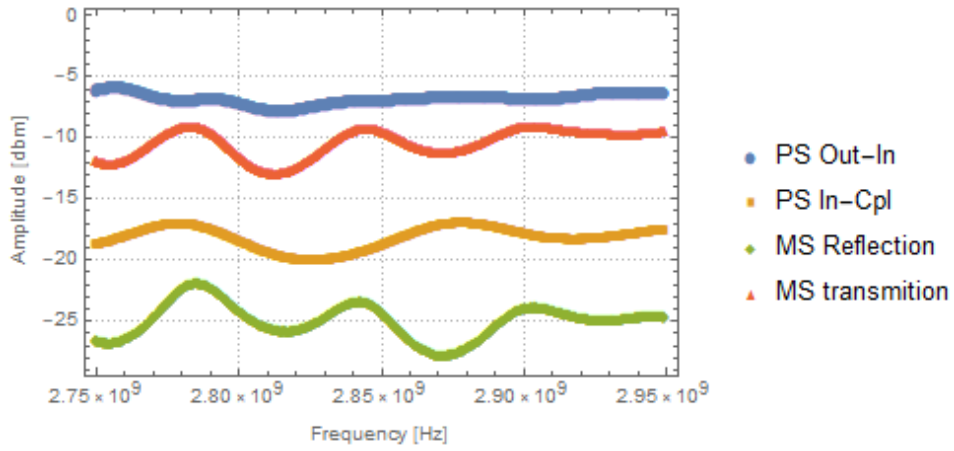


**Figure 2:** Attenuation od the power at 0dBm from top to bottom:  $T_{CPL}, T_{Cpl-MS}$ ,  $R_{CPL}$  and  $R_{Cpl-MS}$



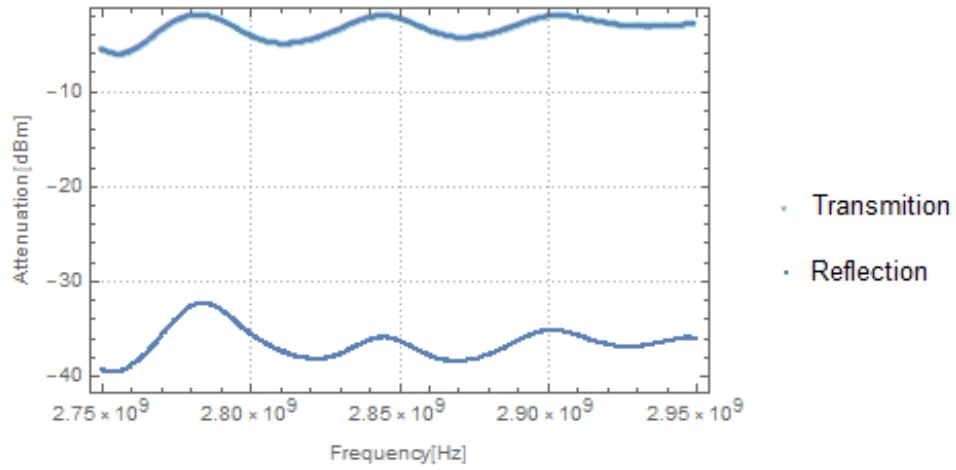


**Figure 3:** Atenuation of the resultant transmtion (top) and reflectrion (bottom) at the Micristrip, at 0dBm in a 2.8GHZ frequency center.

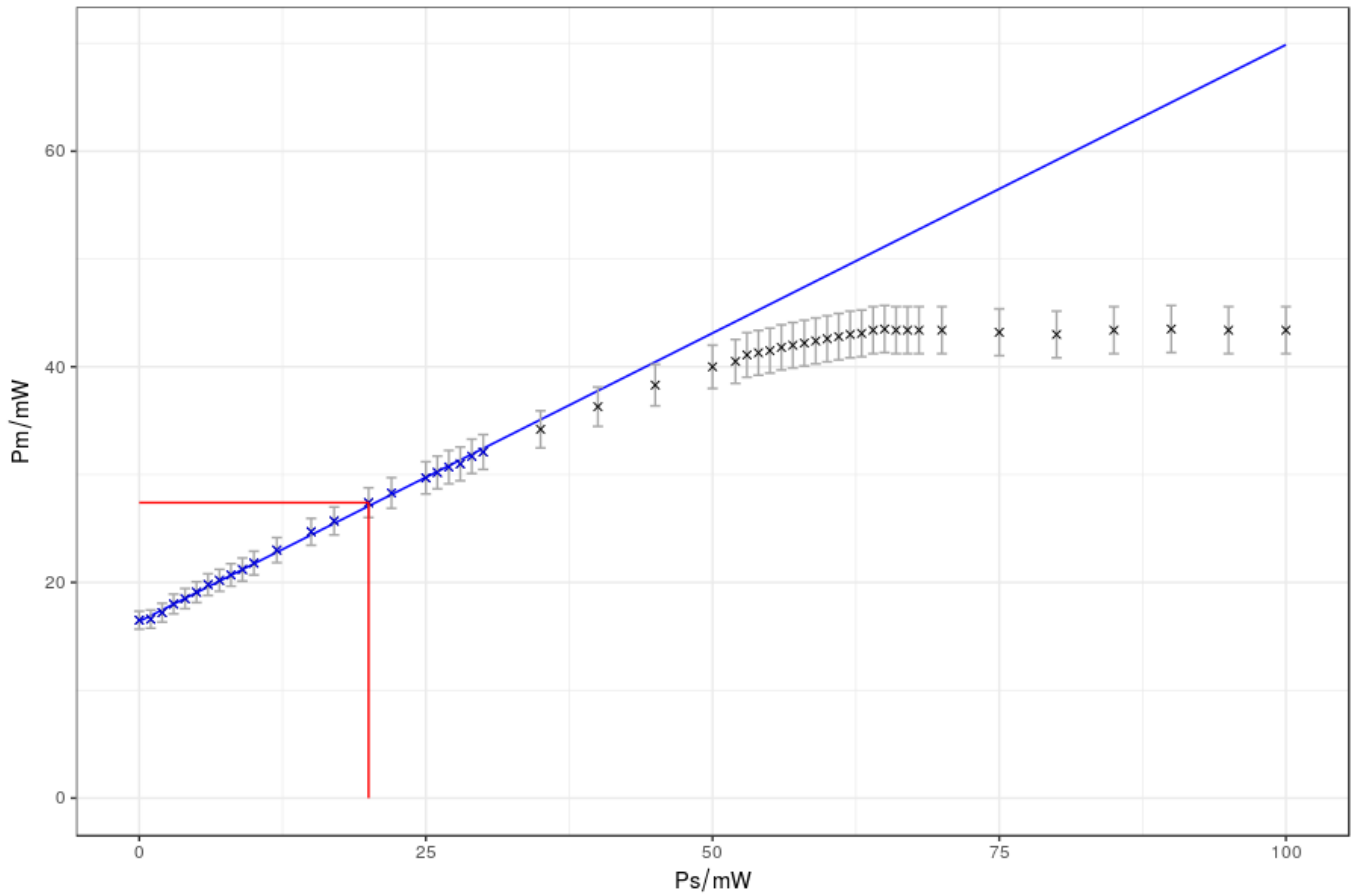


Figure 4: Measurement of the laser power

## 4 Evaluation

### 4.1 Calibration

#### 4.1.1 Laser Power

#### 4.1.2 Optical Spectrometer

#### 4.1.3 ODMR calibrations

#### Shielding

Peak	Position	Element	Position [fraunhoferlines]	Difference
1	$526.8 \pm 1.7$	Fe I	527.0	-0.2
2	$590.0 \pm 0.5$	Na I	589.6	+0.4
3	$628.9 \pm 0.3$	Fe I	630.3	-1.4
4	$657.2 \pm 0.3$	H $\alpha$	656.3	+0.9
5	$688.6 \pm 0.5$			
6	$763.5 \pm 1.3$			
7	$824.7 \pm 0.3$			

Table 1: Positions of the Fraunhofer Lines compared to the literature values

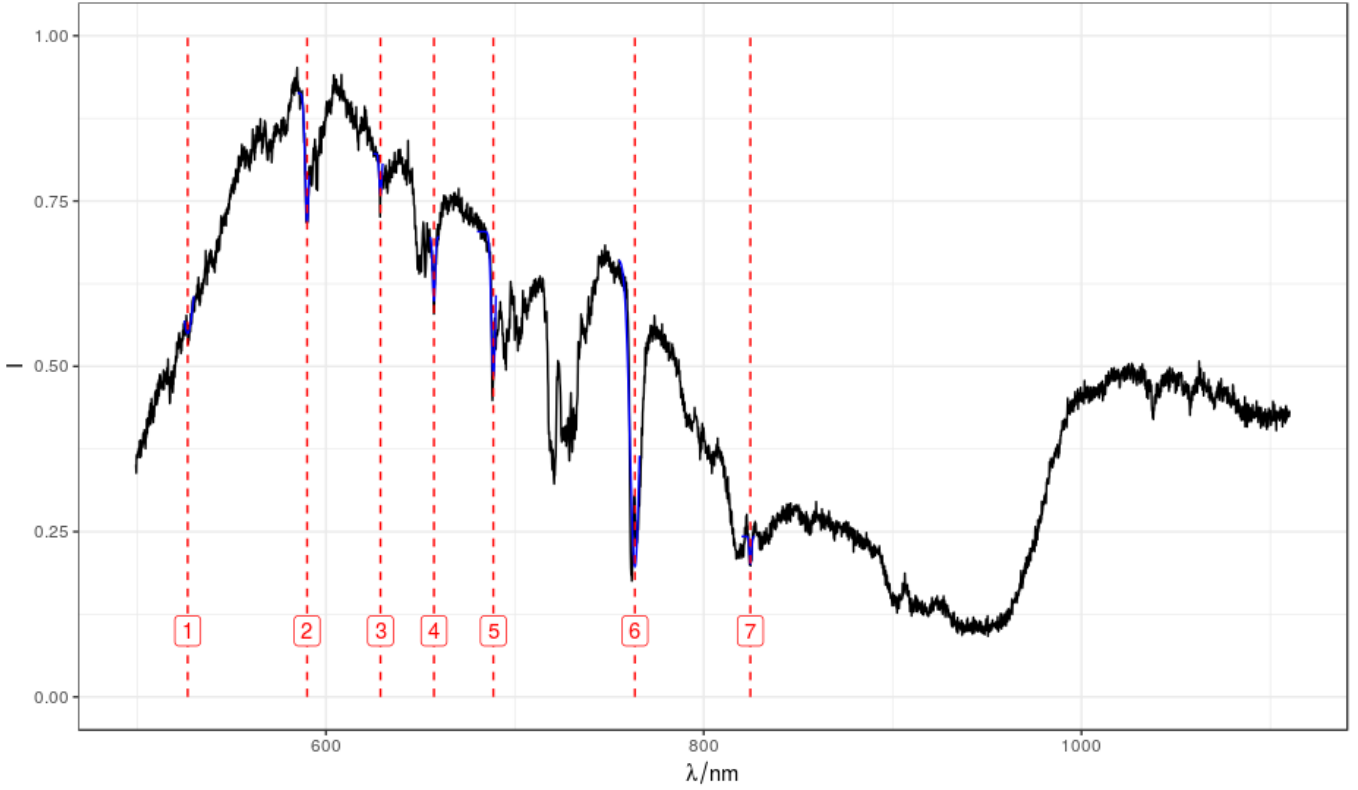


**Figure 5:** Spectrum of the sun with identified Fraunhofer lines for calibration of the optical spectrometer

**Time-to-Frequency Conversion** Performing ODMR measurements we achieve the ODMR spectra on the oscilloscope. Therefore the spectra are time-resolved. To gain frequency-resolved spectra we need to calculate the conversion factor from time to frequency. We do this by performing two sweeps with shifted centre frequencies which allows us to calculate the conversion factor and also the offset since we know the frequency at which the peak appears.

The conversion can be expressed by the following equation:

$$f(t) = \frac{f(t_1)(t_1 - t_2) - (f(t_1) - f(t_2))t_1}{t_1 - t_2} + \frac{f(t_1) - f(t_2)}{t_1 - t_2} \cdot t \quad (3)$$

Inserting the values achieved from figure 8 we get the following conversion function:

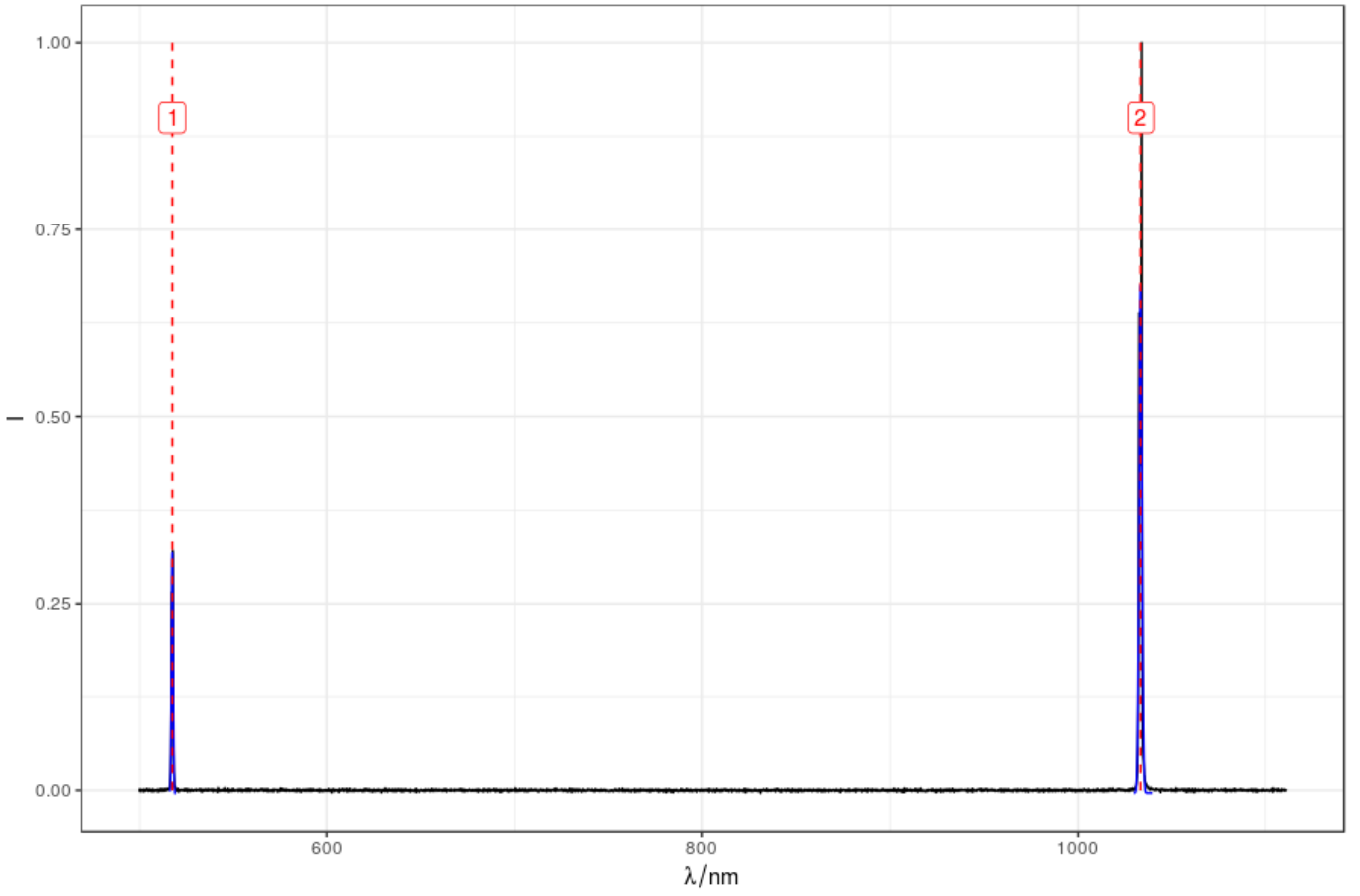
$$f(t) = (1.003 \pm 0.003) \frac{\text{GHz}}{\text{s}} \cdot t + (2.708 \pm 0.011) \text{ GHz} \quad (4)$$

Later in this document all spectra are converted by this function and therefore shown in the frequency domain. The errors are gained from the fit and propagated using Gaussian error propagation.

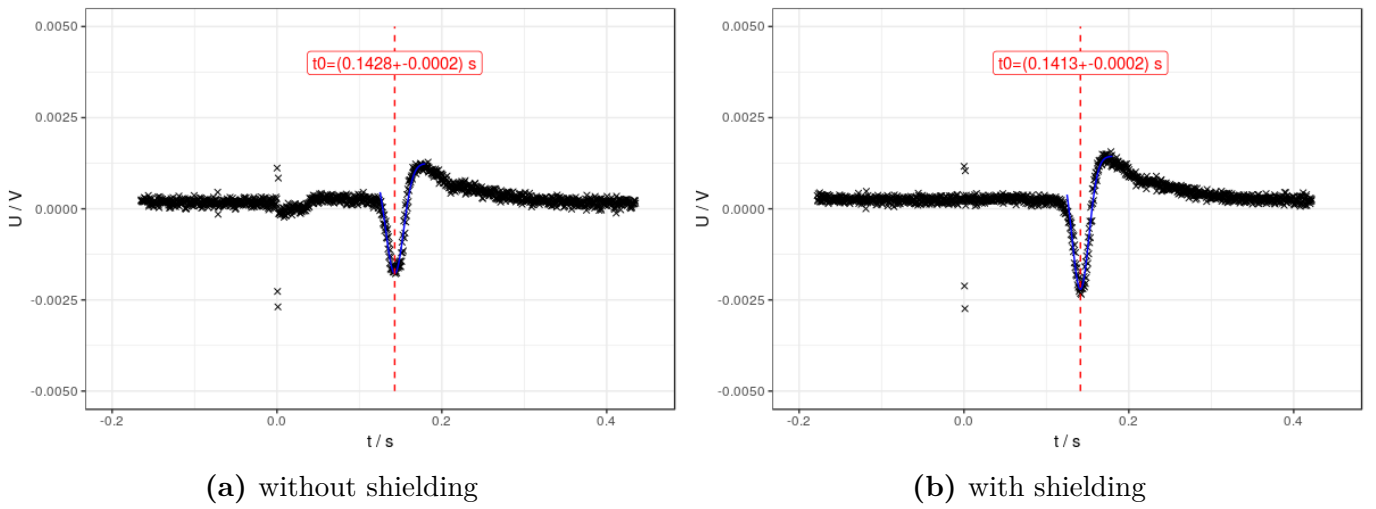
## 4.2 Size of the Diamonds

## 4.3 Fluorescence Spectrum

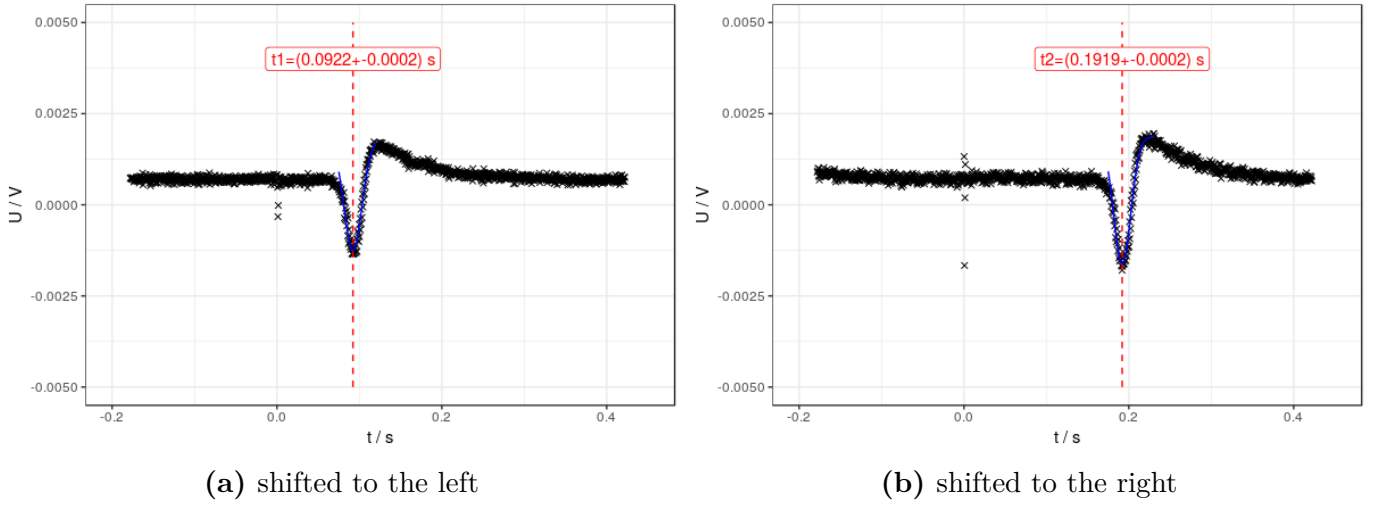
## 4.4 ODMR Measurements



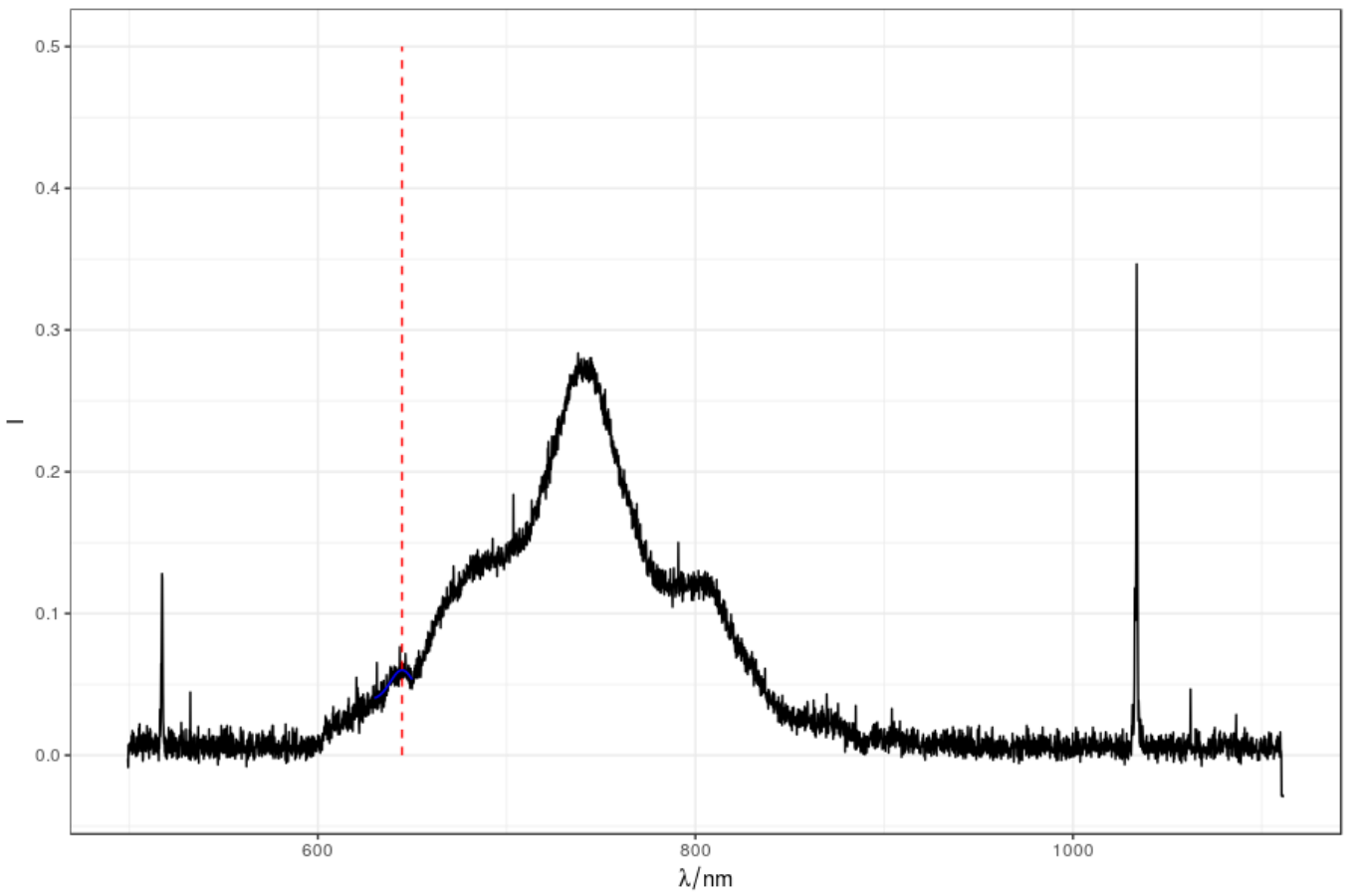
**Figure 6:** Spectrum of the laser with identified peaks at the wavelengths  $\lambda = (517.3 \pm 0.2) \text{ nm}$  and  $\lambda = (1033.7 \pm 0.4) \text{ nm}$



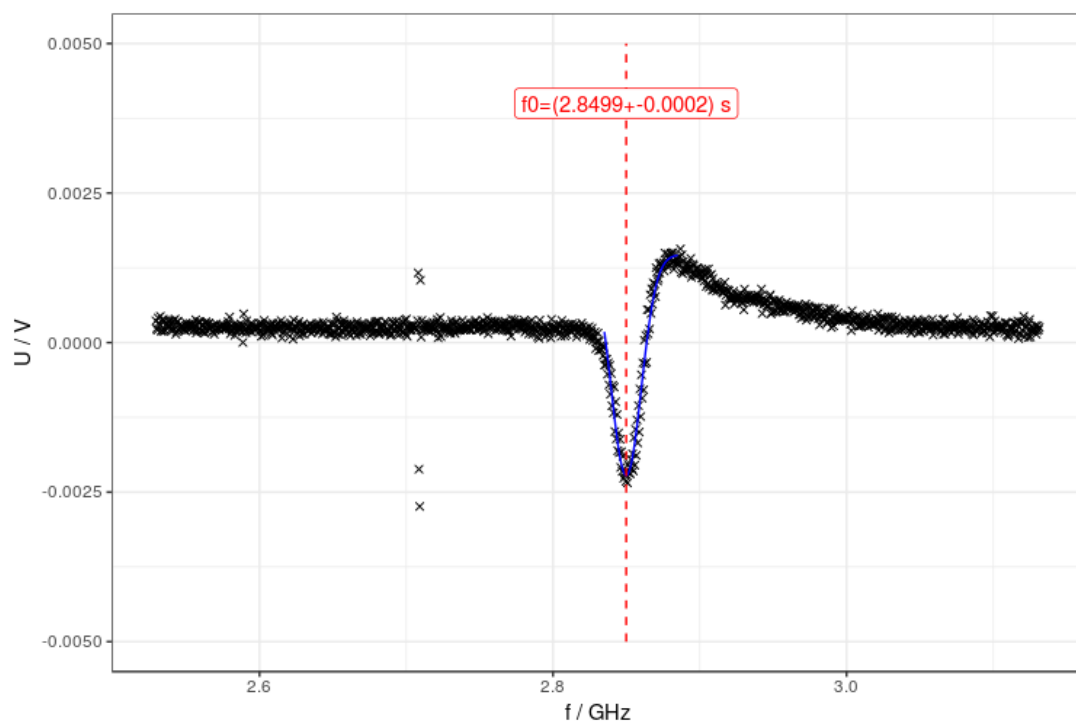
**Figure 7:** ODMR spectrum



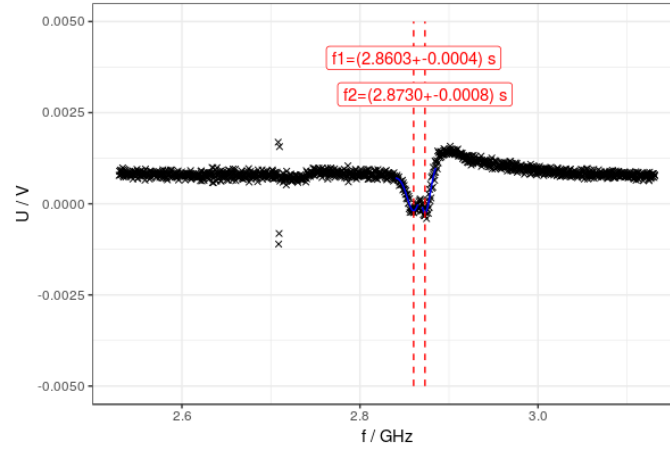
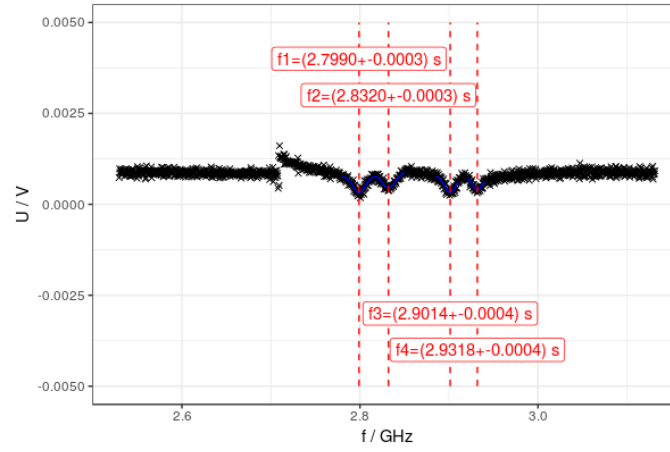
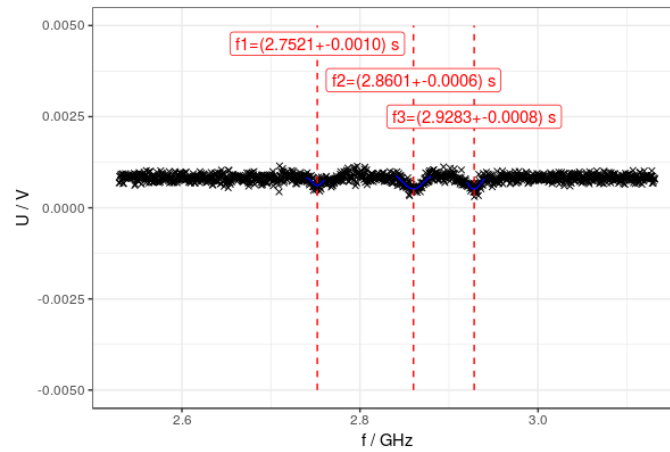
**Figure 8:** ODMR spectrum for time-to-frequency calibration



**Figure 9:** Fluorescence spectrum of the diamond with the zero phonon line (red line) at  $\lambda = (645 \pm 3)$  nm. The spectrum was achieved by averaging over 10 measurements.



**Figure 10:** ODMR Measurement of the diamond without a magnetic Field

(a) Magnetic field in  $x$ -Direction(b) Magnetic field in  $y$ -Direction(c) Magnetic field in  $z$ -Direction**Figure 11:** ODMR spectrum within a magnetic field

## 5 Summary and Discussion



## 6 Appendix

## List of Figures

1	diferent arranges of the CPL and MicroStrip conected to the DSA . . . . .	4
2	Atenuattion od the power at 0dBm from top to bottom: $T_{CPL}, T_{Cpl-MS}$ , $R_{CPL}$ and $R_{Cpl-MS}$ . . . . .	4
3	trans-refl . . . . .	5
4	Measurement of the laser power . . . . .	6
5	Spectrum of the sun with identified Fraunhofer lines . . . . .	7
6	Spectrum of the laser . . . . .	8
7	ODMR spectrum . . . . .	8
8	ODMR spectrum for time-to-frequency calibration . . . . .	9
9	Fluorescence spectrum of the diamond . . . . .	9
10	ODMR Measurement of the diamond without a magnetic Field . . . . .	10
11	ODMR spectrum within a magnetic field . . . . .	11

List of Tables

1     Positions of the Fraunhofer Lines compared to the literature values   . . . . . 6